

TeraPool-SDR: An 1.89TOPS 1024 RV-Cores 4MiB Shared-L1 Cluster for Next-Generation Open-Source Software-Defined Radios

Yichao Zhang
yiczhang@iis.ee.ethz.ch
Integrated Systems Laboratory
ETH Zürich
Zürich, Switzerland

Marco Bertuletti
mbertuletti@iis.ee.ethz.ch
Integrated Systems Laboratory
ETH Zürich
Zürich, Switzerland

Samuel Riedel
sriedel@iis.ee.ethz.ch
Integrated Systems Laboratory
ETH Zürich
Zürich, Switzerland

Matheus Cavalcante
matheusd@iis.ee.ethz.ch
Integrated Systems Laboratory
ETH Zürich
Zürich, Switzerland

Alessandro Vanelli-Coralli
avanelli@iis.ee.ethz.ch
Integrated Systems Laboratory
ETH Zürich
Zürich, Switzerland
Università di Bologna
Bologna, Italy

Luca Benini
lbenini@iis.ee.ethz.ch
Integrated Systems Laboratory
ETH Zürich
Zürich, Switzerland
Università di Bologna
Bologna, Italy

ABSTRACT

Radio Access Networks (RAN) workloads are rapidly scaling up in data processing intensity and throughput as the 5G (and beyond) standards grow in number of antennas and sub-carriers. Offering flexible Processing Elements (PEs), efficient memory access, and a productive parallel programming model, many-core clusters are a well-matched architecture for next-generation software-defined RANs, but staggering performance requirements demand a high number of PEs coupled with extreme Power, Performance and Area (PPA) efficiency. We present the architecture, design, and full physical implementation of TeraPool-SDR, a cluster for Software Defined Radio (SDR) with 1024 latency-tolerant, compact RV32 PEs, sharing a global view of a 4 MiB, 4096-banked, L1 memory. We report various feasible configurations of TeraPool-SDR featuring an ultra-high bandwidth PE-to-L1-memory interconnect, clocked at 730 MHz, 880 MHz, and 924 MHz (TT/0.80 V/25 °C) in 12 nm FinFET technology. The TeraPool-SDR cluster achieves high energy efficiency on all SDR key kernels for 5G RANs: Fast Fourier Transform (93 GOPS/W), Matrix-Multiplication (125 GOPS/W), Channel Estimation (96 GOPS/W), and Linear System Inversion (61 GOPS/W). For all the kernels, it consumes less than 10 W, in compliance with industry standards.

CCS CONCEPTS

• **Computer systems organization** → **Multicore architectures**;
• **Hardware** → **Digital signal processing**; • **Networks** → *Topology analysis and generation*.

KEYWORDS

Many-core, RISC-V, Software-Defined Radios, Physical Design

1 INTRODUCTION

Implementing the 5th-Generation (5G) Radio Access Networks (RAN) standards and beyond, requires flexible high-performance

computing systems that can sustain large computational workloads and memory footprints in a tight power envelope. To guarantee time-to-market and performance, industry is moving from architectures where network functions are offloaded to specialized accelerators to an open and disaggregated Software Defined Radio (SDR) paradigm [9], building processing pipelines as a chain of programmable components. Off-the-shelf products include programmable [3, 8, 10] or reconfigurable [12] hardware with their in-house software libraries. Their designs target 10 Gbps uplink bandwidth at less than 50 W power consumption [3, 10], on Fast Fourier Transform (FFT) for Orthogonal Frequency Division Multiplexing (OFDM), Matrix Multiplication (MatMul) for Beam Forming (BF), Channel Estimation (CHE), and Linear System Inversion (SysInv) for Multiple-Input, Multiple-Output (MIMO) detection: the big heterogeneous workloads of the 7.X Open Radio Access Networks (O-RAN) functional splits [7]. However, closed proprietary does not allow open research, community-based hardware-software co-design, a propulsive force for SDRs.

Focusing on programmable solutions, the many-core cluster offers energy-efficient parallelism. A successful architectural pattern is shared-L1 cluster that eliminates the hardware and software overheads incurred by replicating a private-L1-base many-core cluster for performance purposes [2, 4] (synchronization, inter-cluster data allocation-splitting, and workload distribution among clusters). Increasing the shared memory many-core cluster scale is also highly desirable to exploit the embarrassingly parallel features of SDR processing. Focusing on a concrete example, the parallelization of 5G Physical Uplink Shared Channel (PUSCH) receiver processing [1] exhibits strong data dependencies: for instance, different FFT streams of the OFDM stage need to be merged and multiplied by a matrix of coefficients in the BF stage. If a single cluster shared-L1 is not large enough, MatMuls can be tiled, but the OFDM data must first be merged through the upper levels of the memory hierarchy. Table 1 resumes this data transfer overhead for each stream, comparing four loosely-coupled 1 MiB clusters and a single shared-L1 4 MiB cluster, working on 64 OFDM-antennas of 3276-subcarriers

and a $32 \times 64 \times 3276$ BF MatMul. In the first case, the 32 b words 64 OFDM-antennas are divided into groups of 16, the output is transferred to L2 and the MatMul is tiled over rows for each processing streams. In the second, the 64 antennas are all processed in L1 and the MatMul stage only requires the transfer of coefficients.

Table 1: The data transfer for 5G PUSCH in different clusters.

	1 MiB Clusters	4 MiB Cluster
#Clusters×Cores	4×256	1×1024
(OFDM-antennas×subcarriers)/Cluster	16 × 3276	64 × 3276
BF(MatMul) Size/Cluster	32 × 64 × 819	32 × 64 × 3276
Max. L1-occupation (KiB)	520	2055
Transfer-out OFDM-antennas (KiB)	205	-
Transfer-in BF-inputs (KiB)	213	8
Total Transfer Overhead (KiB)	418	8

The existing many-core cluster only up to tens complex processors with shared L1 space: Kalray’s MPPA-256 features a 16-cores shared 2 MiB cluster-based architecture, Esperanto ET-SoC-1’s 4 MiB L1 are shared by 32 vector cores and Ramon RC64 has 64 cores with 4 MiB shared memory [2, 4, 5], which are not scalable to the parallel processing of 5G O-RAN large problems. The OFDM and BF are indeed very compute-intensive steps. With N_{SC} subcarriers, N_R antennas, N_B beams, the computational complexity of the kernels is $O(N_R \times N_{SC} \log(N_{SC}) + N_R \times N_{SC} \times N_B)$ real Multiply Accumulate (MAC) operations. In PUSCH, up to 14 FFT & MatMul streams are executed per 1ms Transition Time Interval (TTI), which in a typical use-case ($N_{SC} = 3276$, $N_B = 32$), takes ~ 0.8 TOPS with 64 receivers (5G) and ~ 1.8 TOPS with 128 (6G) receivers. This requires a scalable cluster with thousands of programmable agile cores, running at near GHz frequency.

This work introduces TeraPool-SDR, a peak 1.89 TOPS cluster, featuring 1024 RISC-V cores with hierarchical low-latency interconnections to a fully shared 4 MiB, 4096-banked L1 Scratchpad Memory (SPM). The contributions are:

- A physical-aware architecture design for O-RAN workloads, based on a three-level physical implementation hierarchy: the Tile, the SubGroup, and the Group;
- A detail latency-throughput evaluation of on-chip Non-Uniform Memory Access (NUMA) latency interconnection;
- A complete physical implementation and Power, Performance and Area (PPA) analysis of each design configuration, using the cutting-edge 12 nm FinFET technology node;
- A comprehensive performance and energy efficiency evaluation on key 5G-SDR kernels, showing 0.18–0.84 TOPS and 60–125 GOPS/W in real 5G 7.X split benchmarks, meets the O-RAN specifications and is the first open-sourced¹ programmable solution for complete physical layer processing.

2 ARCHITECTURE

While it was demonstrated that shared-L1 clusters with up to 256 cores can be built [11], their performance is still insufficient for

¹<https://github.com/pulp-platform/mempool>

low-latency TTI 5G pipelines. To meet real-life O-RAN requirements, TeraPool-SDR needs to “enter into uncharted territories” in terms of core count, aiming at a 4x increase over the largest cluster reported in the literature. We must aggressively leverage physical design awareness, building the cluster hierarchically to ensure high Processing Elements (PEs)-L1 bandwidth and energy efficiency.

2.1 Snitch Core, Tile and Interconnection

TeraPool-SDR’s PEs are single-stage 32-bit RISC-V *Snitch* cores [13] featuring an accelerator port to offload complex instructions to pipelined functional units. Our Snitch supports the RV32IMAXpulp² Instruction Set Architecture (ISA) and multiple outstanding transactions to tolerate multi-cycle memory access latencies. Snitch retires loads out-of-order, yet delivers in-order data to the execution units.

The basic building block of TeraPool-SDR is the *Tile*, Figure 1. It contains 8 Snitch PEs, with a 32 instructions private L0 Instruction Cache (I\$) each, and a shared 4 KiB two-way set-associative L1 I\$. The PEs are tightly coupled to 32 1 KiB data Static Random-Access Memory (SRAM) L1 banks. The Advanced eXtensible Interface (AXI) master port, used for L1 I\$ refill, and Direct Memory Access (DMA) transfers, for data-intensive applications, is shared between all the cores.

A hierarchical topology is essential for an implementable interconnection between 1024 PEs and 4096 memory banks. To keep low-latency Tightly Coupled Data Memory (TCDM) access, we implement Fully-Connected (FC) logarithmic crossbars and arbiters within each design level to have purely combinational routing. Pipeline registers are optionally added at hierarchy boundaries to reduce critical paths in the physical design at the cost of increased latency. Separate request (address, data write, and control) and response (request ID, data read, and acknowledgment) networks then handle NUMA accesses.

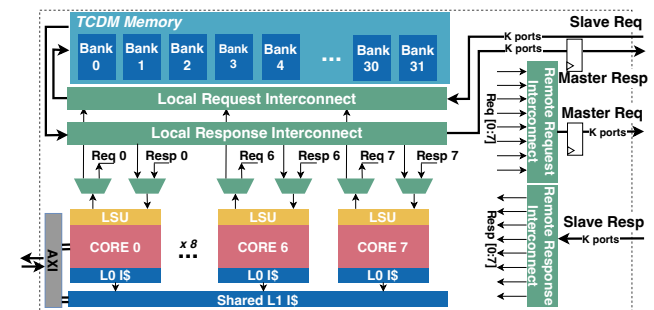


Figure 1: The TeraPool-SDR Tile architecture, the FC crossbar interconnections protocol specified in Section 2.1.

At the Tile level, PEs are connected to the local portion of the cluster’s shared SPM with a FC crossbar, providing single-cycle zero-load access latency. Each Tile has a parameterizable number of remote ports to route requests to other Tiles’ SPM banks via the *remote request interconnect*. Corresponding responses are routed to the core on the *remote response interconnect*. To access the SRAM

²The Xpulping extension includes domain-specific instructions [11], e.g., MAC and load-post-increment.

banks, incoming requests directly connect to the Tile FC local crossbar. The local interconnect provides a master port for each of the K incoming request ports, resulting in an $(8 + K) \times 32$ crossbar.

2.2 Cluster Configurations

The TeraPool-SDR Cluster consists of 128 Tiles, including 1024 Snitch cores and 4096 1 KiB SRAM banks of L1 SPM. Choosing the hierarchies and the placement of the interconnects within, strongly conditions the design feasibility. For example, a single upper hierarchy with 128 Tiles connected by a 128×128 crossbar is clearly unfeasible. Grouping 16 Tiles results in $K = 8$ ports per Tile (one for each Tile-Group) and delivers high inter-Tile interconnect bandwidth. However, it requires eight 16×16 FC crossbars within the hierarchy level, and leads to unmanageable routing congestion. Moreover, it is impossible to place the 8 Tile-Groups in a grid that results in balanced, short access paths and the Electronic Design Automation (EDA) runtime for the Tile-Group design iteration is unmanageable. More details on physical feasibility are shown in Section 3.

To make such a huge cluster physically feasible, we propose the following design strategies for the TeraPool-SDR architecture:

- (1) The topmost hierarchy, the Group, is replicated 4 times and arranged in a 2×2 grid to both shorten and balance the diagonal access paths between the Groups.
- (2) To keep the EDA tool’s runtime manageable, a Group is divided into multiple finely-tuned physical implementation hierarchies. That is, each Group consists of 4 SubGroups, and each SubGroup contains 8 Tiles.
- (3) Targeting high inter-tile bandwidth, we forward Tiles’ remote Group requests directly to the Group level, where we implement 32×32 FC crossbars for each target Group.

Given the interconnect required to establish local connections among Tiles in a SubGroup, we partition the local interconnection among the four SubGroups, equipping each with four 8×8 FC crossbars, improving physical routing feasibility. A Tile’s remote request is routed based on the targeted hierarchy: local SubGroup, remote SubGroups, or remote Groups, resulting in $K = 7$ ports: 1 connects locally to other Tiles in the same SubGroup via a 8×8 FC crossbar, 3 connect to Tiles in the other 3 SubGroups within the local Group via three 8×8 FC crossbars, and 3 connect to Tiles in the other 3 remote Groups via three 32×32 crossbars.

The hierarchy levels provide flexibility to place pipeline registers and break long remote access paths. Within the Group, registers are placed at each hierarchy boundary on master ports. The latency between Groups is a hardware-parameter that trades off the target operating frequency and latency. We call those parametrizations **TeraPool-SDR_{1-3-5-X}** architecture, where the subscripts indicate the zero-load cycle latency for core access at each hierarchy level, i.e., Tile, SubGroup, Group, Cluster. The **TeraPool-SDR₁₋₃₋₅₋₅** design has no extra registers between the two Groups. A register is added on both request and response paths between Groups at the Cluster level in the **TeraPool-SDR₁₋₃₋₅₋₇** design, increasing the round-trip latency by 2 cycles. In **TeraPool-SDR₁₋₃₋₅₋₉** and **TeraPool-SDR₁₋₃₋₅₋₁₁**, additional spill registers are added respectively to slave or both master-slave ports of the Group hierarchy level. The maximum access latency increases by 4 and 6 cycles. As

an example, the full architecture overview of TeraPool-SDR₁₋₃₋₅₋₇ is shown in Figure 2. These configurations create a trade-off between achievable frequency and L1 worst-case latency. A cluster-level AXI interface is available for connection with external peripherals, chosen depending on the system design, which is not discussed in this paper.

2.3 Interconnection latency-throughput trade-off

To compare the performance of various topologies, we replace the cores with traffic generators producing memory requests following a Poisson process with a rate λ and targeting random and uniformly distributed destination banks. We present the latency and throughput as a function of the injected load, measured in requests per core per cycle.

As shown in Figure 3 left, the throughput exhibits a linear-increasing trend until saturation, as the injected requests start conflicting in the interconnect to the L1 banks. Increasing the number of pipeline registers creates a deeper interconnection that accepts more requests before generating conflicts. Therefore, the saturation load ranges 0.23-0.245 request/core/cycle. Figure 3 right shows the average round-trip latency of a memory request. For a low injected load, the simulated latency asymptotically approaches the zero-load access latency, ranging from 4.9 to 9.3, depending on the configuration. As the injected load increases, the average latency grows, its asymptotic knee going from 10 to 14 (40% variation) and corresponds to throughput saturation, at the interconnect congestion. This analysis shows a clear trade-off between latency and throughput of different configurations. However, random loads generate an adverse access pattern with no locality within Tiles. We analyze performance on key O-RAN application kernels in section 4.

3 PHYSICAL IMPLEMENTATION

We implement TeraPool-SDR with GlobalFoundries’ 12 nm LPPLUS FinFET technology, using Synopsys’ Fusion Compiler 2022.03 for synthesis, Place and Route (PnR), determining the power consumption by Synopsys’ PrimeTime 2022.03 under typical operating conditions (TT/0.80 V/25 °C) with switching activities obtained from post-PnR gate-level simulations with back-annotated parasitic information. We use a bottom-up implementation flow, creating abstract design views during assembly, including only interface logic and register timing information, to reduce the EDA runtime.

3.1 Floorplan and Feasibility

We show TeraPool-SDR physical design full view in Figure 4. To fully leverage the available Back-End-of-Line (BEOL) resources and ease interconnect routing through Tiles without manual port placement, we flatten the Tile in the SubGroup, obtaining a $1.52mm \times 1.52mm$ area with a satisfactory utilization of 55%, as the first implementation hierarchy level. The SPM macros of each Tile are grouped and arranged in a U-shape to enclose the local crossbar, minimizing overall distance and avoiding excessive stacking of macros. SubGroup and Group blocks are arranged in a point-symmetric grid to balance the diagonal access paths, with channels in between

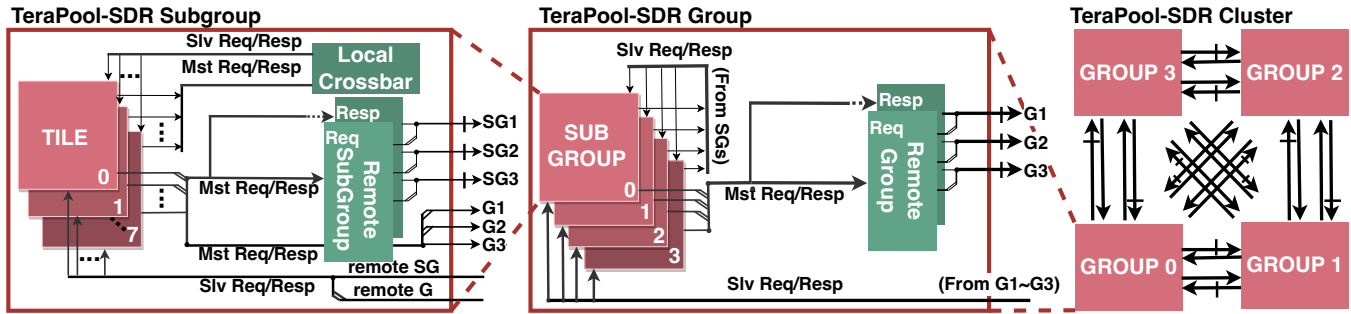


Figure 2: Bottom-up architecture of TeraPool-SDR₁₋₃₋₅₋₇, with the interconnection protocol specified in Section 2.1.

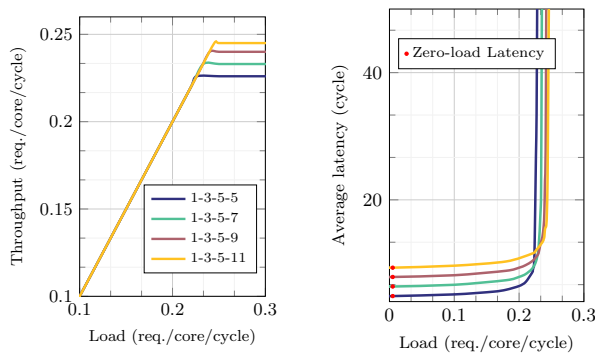


Figure 3: Throughput and average round-trip latency of TeraPool-SDR's L1 interconnect as a function of the load.

to place and route the interconnects. To further improve area utilization, we place interface ports behind the SubGroup blocks and shrink the channel width until BEOL resources become limited.

The runtime of EDA tools serves as a fundamental indicator of both the design optimization effort and viability [14]. As mentioned in Section 2.2, although the Cluster configuration comprising 8 Groups with 16 Tiles each delivers high inter-Tile interconnect bandwidth, it is not physically feasible. The trail implementation shows total EDA runtime of this configuration is nearly $3.5\times$ that of TeraPool-SDR₁₋₃₋₅₋₉, with timing optimization accounting for more than 80% of the effort, and the routing stage is $5.5\times$ slower than the other configurations. Despite these high design optimization efforts, the eight 16×16 interconnects in this Group design generate significant routing congestion and numerous metal shorts in the post-routing design phase. Furthermore, routing detours considerably increase the length of timing paths, making it impossible to close the design with a 500 MHz target frequency, under typical operating conditions (TT/0.80 V/25 °C). All TeraPool-SDR configurations are physically feasible.

3.2 Peak-Performance & Area

Table 2 presents the post-PnR peak-performance & area results for the most promising TeraPool-SDR configurations, in comparison

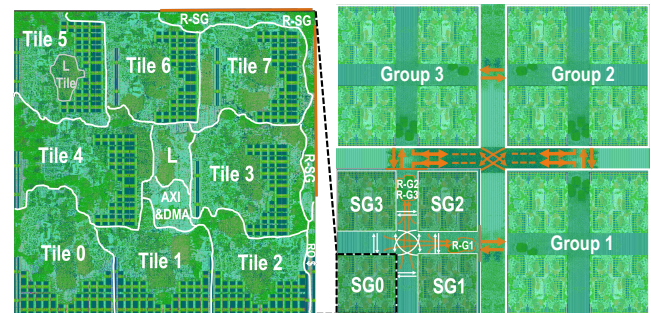


Figure 4: Placed-and-routed layout annotated view of each TeraPool-SDR hierarchical instance.

to a smaller-scale, 256-core MemPool design in the same technology node. For fair comparison, we keep 55% area utilization on the base hierarchy of all the implementations. TeraPool-SDR organizes wisely hierarchical interconnects that contribute minimal area overhead, accounting for only 8.5% of the total design area. TeraPool-SDR breaks the TOPS wall, achieving peak performance comprised between 1.50 TOPS and 1.89 TOPS, depending on the latency configuration. Although a large-scale physical design leads to longer distance paths, TeraPool-SDR's low-latency scheme still keeps a small Fan-Out-of-4 (FO4) delay. When the configured latency exceeds 11 cycles, the operating frequency is no longer constrained by the remote Group access path but by the Snitch core: the critical path, consisting of only 63 logic levels, starts at a register after the instruction cache, passes through Snitch and a request interconnection, and arrives at the clock gating of an SRAM bank. On the top hierarchy, TeraPool-SDR loses area efficiency due to the large 32×32 interconnection modules in each Group, requiring more routing area, and the difficult routing of feedthrough connections across Groups, caused by the blocking SubGroups placement. These challenges impose physical constraints on the further scaling of shared-L1-memory architectures beyond the 1000-cores milestone. We nevertheless believe that exploring 3D-IC solutions will be beneficial for future research [6].

4 SDR BENCHMARKS PERFORMANCE

TeraPool-SDR offers a streamlined fork-join programming model, highly suitable for hardware-software co-design of SDR workloads.

Table 2: Post-PnR peak-performance & area results.

	MemPool ₂₅₆ [*]	TeraPool-SDR ₁₀₂₄ [*]		
	1-3-5	1-3-5-7	1-3-5-9	1-3-5-11
Hier. Access Latency [cycle]				
Area [mm ²]	10.0	68.9	68.9	68.9
Area Per Core [mm ² /core]	0.039	0.067	0.067	0.067
Logic Gate [MGE]	44	176	176	176
Logic Gate Per Core [MGE/core]	0.17	0.17	0.17	0.17
TCDM Spill Register in Group	✓	✓	✓✓	✓✓✓
TCDM Spill Register in Cluster	-	✓	✓	✓
Operating Frequency (<i>Worst</i>) [MHz]	728	530	637	740
Operating Frequency (<i>Typ.</i>) [MHz]	915	730	880	924
Logic Delay [FO4]	162.4	204.5	169.8	161.2
Max Throughput [req/core/cycle]	0.33	0.23	0.24	0.25
Avg. Latency (<i>Zero-load</i>) [cycle]	4.7	6.4	7.9	9.3
Peak Performance (<i>Typ.</i>) [TOPS]	0.47	1.50	1.80	1.89
Area Efficiency [GOPS/mm ²]	47.0	21.8	26.1	27.4

^{*} Subscript indicates core count; implemented in GF12LP+ technology.

Targeting optimized architecture-native kernel libraries, we adopt a low overhead C-runtime approach and distribute portions of the input data to the PEs, according to their ID (accessible via runtime primitives). After a parallel-section cores are synchronized with a runtime barrier call. To keep utilization high and avoid contentions to shared memory resources, PEs are constrained to fetch data from portions of the shared SPMs they can access with low latency. Key kernels for SDR workloads are implemented: FFT, beamforming MatMul, CHE, and SysInv.

We adopt a radix-4 decimation in frequency Cooley-Turkey FFT, to ease the memory accesses in local banks [1]. In the k^{th} stage of an N-points FFT, each core computes 4 butterflies, taking 4 inputs at a distance of $N/(4 \times 4k)$. Cores working on different FFTs are independently synchronized.

The **MatMul** tiled implementation [1], aims to fully utilize register file in Snitch, maximizing computational intensity. The implementation reduces interconnect stalls, through a cascaded parallelization, where PEs of the same Tile shift the fetch address start point along matrix rows, to avoid contentions for the same Group port.

In **CHE**, consisting of an element-wise matrix division, cores loop across memory rows, compute the fetch-indexes via modulo operations, and only produce the outputs residing in their local banks.

The **SysInv** leverages weak-scaling: as in the lower-PHY the per-subcarrier MIMO has less than 32 transceivers we assign an independent small squared SysInv problem to each core and then synchronize. We use Cholesky Decomposition (CholDec) to invert the linear system, and store the intermediate lower-triangular decomposition in the local memory of the core working on it.

The large capacity of TeraPool-SDR's L1 allows to set up functional pipelines without resorting to L2 accesses to solve the data dependencies between the different steps of lower-PHY processing (e.g., in a typical OFDM workload the data of FFT for up to 64 antennas can be passed to the MatMul beamforming stage with no L2 memory transfers).

Table 3: Performance metrics of SDR key-kernels.

		TP-SDR ₁₋₃₋₅₋₇	TP-SDR ₁₋₃₋₅₋₉	TP-SDR ₁₋₃₋₅₋₁₁
		Max Size in L1	64 × 4096	64 × 4096
FFT	Total Cycles	31 740	32 012	32 272
	IPC	0.75	0.75	0.74
	Max Size in L1	512 × 512	512 × 512	512 × 512
MatMul	Total Cycles	296 995	298 239	301 113
	IPC	0.70	0.69	0.69
	Max Size in L1	4096 32 × 4	4096 32 × 4	4096 32 × 4
CHE	Total Cycles	16 851	17 221	17 601
	IPC	0.66	0.64	0.63
	Max Size in L1	65536 4 × 4	65536 4 × 4	65536 4 × 4
SysInv	Total Cycles	30 539	31 254	31 870
	IPC	0.61	0.59	0.58

^{*} Each core supports 8 outstanding transactions in the each given system.

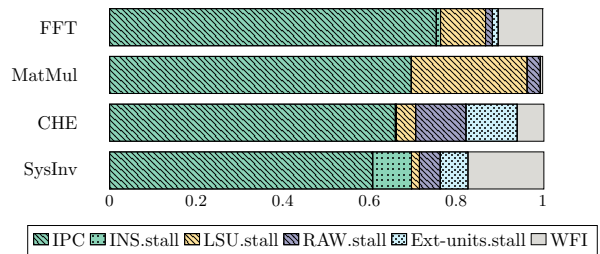
**Figure 5: Fraction of instructions and stalls over the total cycles for the kernels execution in TeraPool-SDR₁₋₃₋₅₋₇.**

Table 3 demonstrates that TeraPool-SDR's large shared-L1 memory enables processing of the entire data frame in a typical 5G use case without splitting, achieving an instructions-per-cycle (IPC) of up to 0.75 for key SDR kernels. TeraPool-SDR's remote Group access latency varies from 7 to 11 cycles, but the IPC loss across different configurations stays below 3%, proving an effective latency-hiding in software and hardware. Figure 5 displays the detailed IPC and stall fractions for the execution of SDR kernels on TeraPool-SDR. The parallelization scheme, minimizes Load Store Unit (LSU) stalls by eliminating access to remote memory banks for FFT, CHE, and SysInv. The read-after-write (RAW) and external-unit stalls in CHE and SysInv result from multi-cycle instructions (mainly divisions) offloaded to pipelined functional units during intensive computing loops. Being a control-heavy task, SysInv experiences more I\$ misses and synchronization overhead. For the MatMul, although target data structures distribute over all the banks of the shared SPM, causing unavoidable LSU stalls, the IPC on the TeraPool-SDR Cluster still achieves 0.7, highlighting that TeraPool-SDR delivers a significant fraction of the peak workload even for kernels with PE-to-L1 traffic patterns that are not highly local, with non-negligible contention.

Figure 6 shows that TeraPool-SDR achieves comparable or higher energy efficiency than a 4× smaller-scale cluster on all the key SDR kernels thanks to its low-power interconnect. TeraPool-SDR₁₋₃₋₅₋₇

is the lowest power consumption design: a memory request crossing the cluster takes 13.5 pJ, only 0.5× more than a local request. The performance and energy efficiency of this design are however dominated by the other two. TeraPool-SDR₁₋₃₋₅₋₁₁ is Pareto-optimal in operating frequency and performance, at the cost of a higher power consumption (6.5 W for FFT, 8.8 W for MatMul, 6.6 W for CHE and 4.9 W for SysInv kernels). With minimal performance losses, TeraPool-SDR₁₋₃₋₅₋₉ is optimal in energy efficiency for the selected SDR workloads. Being the most compute-intensive task, MatMul achieves a peak of 125 GOPS/W and consumes less than 6.4 W, in compliance with the low power consumption standards of base-station hardware.

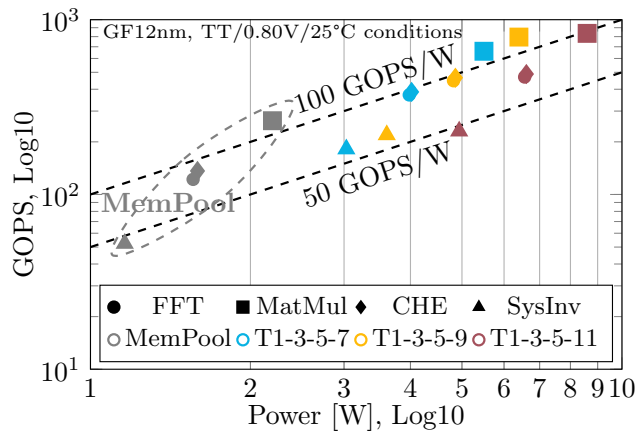


Figure 6: Energy Efficiency for SDR workloads.

5 CONCLUSION

TeraPool-SDR is a physically feasible, many-core cluster of 1024 Snitch RISC-V cores sharing 4 MiB of L1 SPM, through hierarchical low-latency NUMA TCDM interconnections (less than 5 cycles within local Group, 7-11 to remote Group, depending on the target frequency). Completing PnR by using GlobalFoundries' 12LPPLUS FinFET technology, TeraPool-SDR occupies a die area of 68.9 mm² and operates at up to 924 MHz (63 gate delays) in typical operating conditions (TT/0.80 V/25 °C) with a theoretical peak performance of 1.89 TOPS.

TeraPool-SDR's large PE count exceeds the state-of-the-art by 4× and achieves high performance. Depending on the target operating frequencies, TeraPool-SDR achieves 0.18 – 0.84 TOPS and 60 – 125 GOPS/W on the benchmarks of 5G 7.X splits targeted for acceleration in base-station hardware by industry-leading solutions. Thanks to its low-latency interconnect with a large shared-L1, TeraPool-SDR minimizes the data splitting, transfer, and synchronization overheads of memory-intensive SDR applications.

ACKNOWLEDGMENTS

This work is funded in part by the COREnext project supported by the EU Horizon Europe research and innovation program under grant agreement No. 101 092 598.

REFERENCES

- [1] Marco Bertuletti, Yichao Zhang, et al. 2023. Efficient Parallelization of 5G-PUSCH on a Scalable RISC-V Many-Core Processor. In *2023 Design, Automation, and Test in Europe Conference and Exhibition*. IEEE, Antwerp, Belgium, 396–401. <https://doi.org/10.23919/DATE56975.2023.10137247>
- [2] Dave Ditzel, Roger Espasa, et al. 2021. Accelerating ML recommendation with over a thousand RISC-V/Tensor processors on Esperanto's ET-SoC-1 Chip. In *2021 IEEE Hot Chips 33 Symp*. IEEE, Palo Alto, California, 209–220. <https://doi.org/10.1109/HCS52781.2021.9566904>
- [3] EdgeQ. 2023. 5G meets AI. <https://www.edgeq.io/technology/>. Accessed: 11/13/2023.
- [4] Ran Ginosar, David Goldfeld, et al. 2021. Ramon Space RC64-based AI/ML Inference Engine. In *European Workshop on On-Board Data Processing (OBDDP)*. Zenedo, Online, 1–33.
- [5] Ahmed Kamaleldin, Salma Hesham, et al. 2020. Towards a Modular RISC-V Based Many-Core Architecture for FPGA Accelerators. *IEEE Access* 8 (2020), 148812–148826. <https://doi.org/10.1109/ACCESS.2020.3015706>
- [6] Moonsoo Kang. 2023. Heterogeneous Integration Platform for Next Generation Computing. <https://r6.ieee.org/scv-eps/wp-content/uploads/sites/58/2023/02/D2-3-kang.pdf>. Accessed: 2023-11-20.
- [7] Line M. P. Larsen, Aleksandra Checko, et al. 2019. A Survey of the Functional Splits Proposed for 5G Mobile Crosshaul Networks. *IEEE Communications Surveys & Tutorials* 21, 1 (2019), 146–172. <https://doi.org/10.1109/COMST.2018.2868805>
- [8] Marvell. 2023. Data Processing Units (DPU) Empowering 5G carrier, enterprise and AI cloud data infrastructure. <https://www.marvell.com/products/data-processing-units.html>. Accessed: 11/13/2023.
- [9] Joe Mitola. 1995. The software radio architecture. *IEEE Communications Magazine* 33, 5 (1995), 26–38. <https://doi.org/10.1109/35.393001>
- [10] Qualcomm. 2023. How we won the acceleration architecture debate. <https://www.qualcomm.com/news/onq/2023/03/how-we-won-the-acceleration-architecture-debate>. Accessed: 11/13/2023.
- [11] Samuel Riedel, Matheus Cavalcante, et al. 2023. MemPool: A Scalable Manycore Architecture With a Low-Latency Shared L1 Memory. *IEEE Trans. Comput.* 72, 12 (2023), 3561–3575. <https://doi.org/10.1109/TC.2023.3307796>
- [12] Xilinx. 2023. Breakthrough Adaptive Radio Platform for Mass 5G Deployments. <https://www.xilinx.com/products/silicon-devices/soc/rfsoc/zynq-ultrascale-plus-rfsoc-dfe.html>. Accessed: 11/13/2023.
- [13] Florian Zaruba, Fabian Schuiki, et al. 2021. Snitch: A Tiny Pseudo Dual-Issue Processor for Area and Energy Efficient Execution of Floating-Point Intensive Workloads. *IEEE Trans. Comput.* 70, 11 (Nov. 2021), 1845–1860. <https://doi.org/10.1109/TC.2020.3027900>
- [14] Yanling Zhou, Yunyao Yan, et al. 2017. A method to speed up VLSI hierarchical physical design in floorplanning. In *2017 IEEE 12th International Conference on ASIC (ASICON)*. IEEE, Guiyang, China, 347–350. <https://doi.org/10.1109/ASICON.2017.8252484>